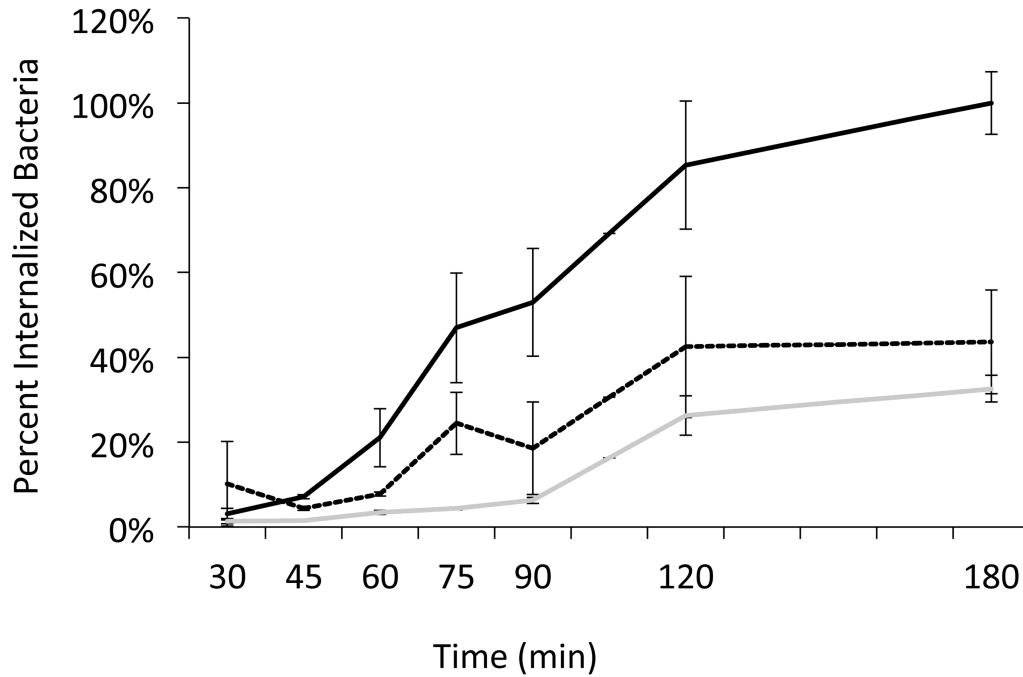


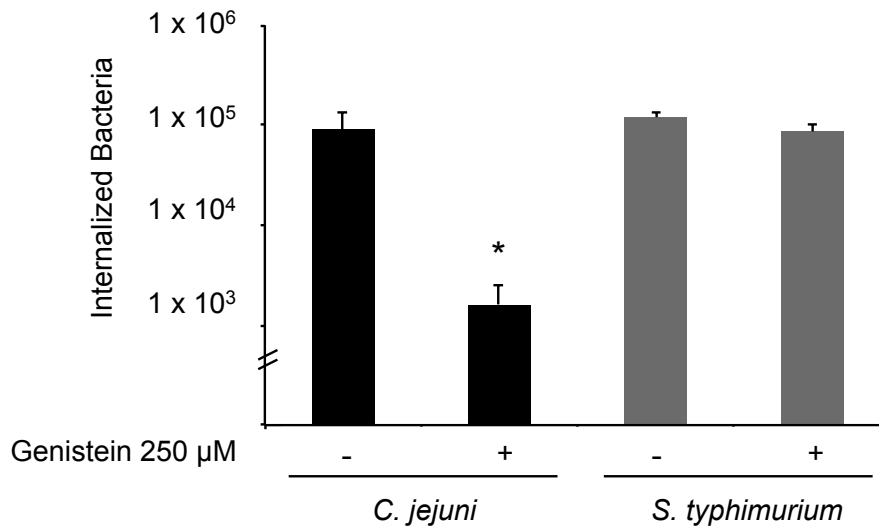
Supporting Materials

S1

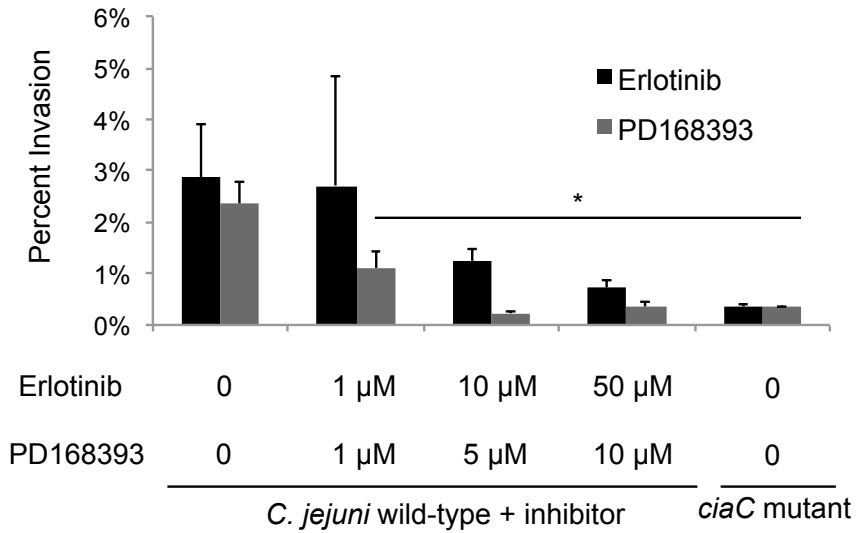


Supplemental Fig. S1. Temporal kinetics of *C. jejuni* internalization by INT 407 cells. Values represent the percent of internalized bacteria/well of a 24-well tissue culture tray relative to the invasion of the *C. jejuni* wild-type stain at 3 hr. Shown are a *C. jejuni* F38011 wild-type strain (solid line, black), *C. jejuni* F38011 wild-type strain treated with 1024 $\mu\text{g/ml}$ of chloramphenicol (dashed line), and the *C. jejuni* *ciaC* mutant (solid line, gray). The error bars represent the standard deviation of the mean of percent internalized bacteria.

S2

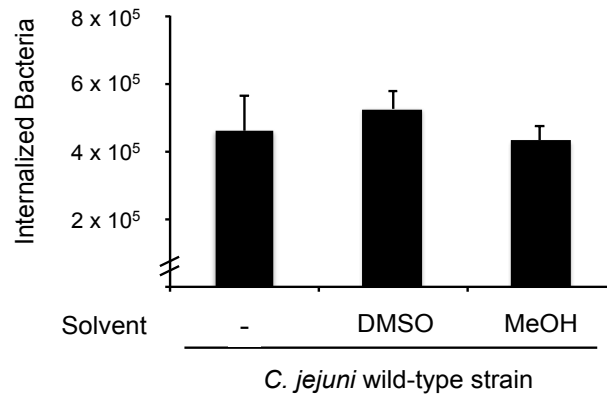


Supplemental Fig. S2. Treatment of INT 407 cells with genistein, a global inhibitor of protein-tyrosine kinases, significantly inhibits *C. jejuni* invasion. The INT 407 cells pretreated with 250 μM of inhibitor 30 minutes prior to inoculation with *C. jejuni* and *S. typhimurium*. The bacteria were incubated with the INT 407 cells for 3 hr prior to gentamicin treatment. Values represent number of internalized (gentamicin-protected) bacteria/well of 24-well tissue culture tray and are given as means of triplicate determinations \pm standard deviations. The asterisk indicates significance ($P < 0.01$) between untreated and genistein-treated samples using the Student's *t* test.



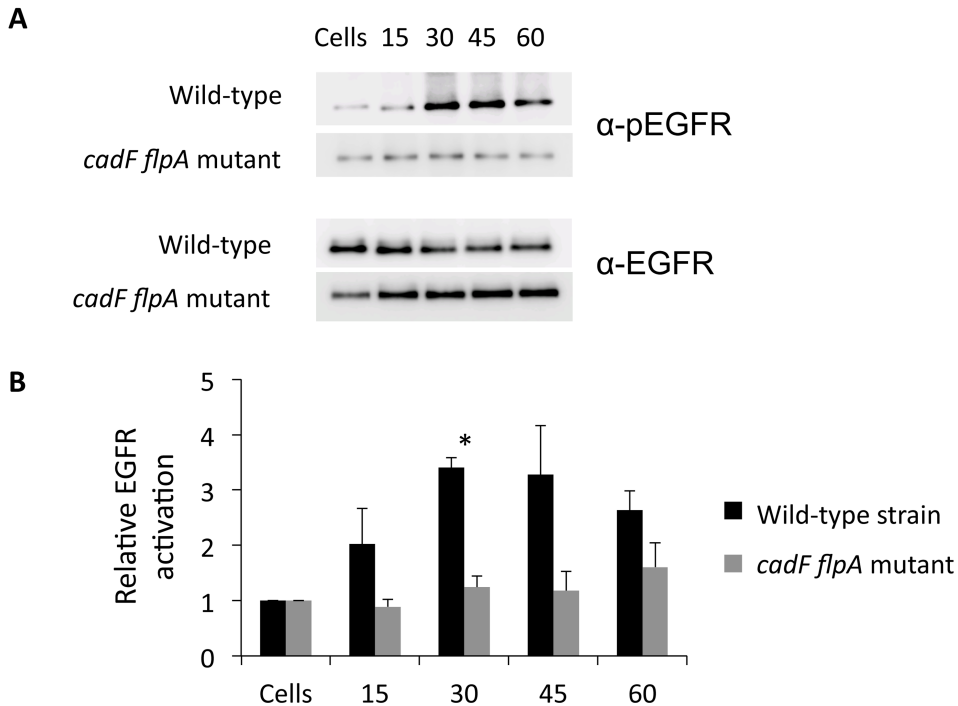
Supplemental Fig. S3. Effect of EGFR inhibitors on *C. jejuni* binding and invasion of INT 407 cells. The INT 407 cells were pretreated with the indicated concentrations of inhibitor 30 minutes prior to inoculation with *C. jejuni*. The bacteria were incubated with the INT 407 cells for 3 hr prior to gentamicin treatment. Values represent number of percent of adherent bacteria that invaded the INT 407 cells. Significance ($P < 0.01$) between samples was determined using Student's *t* test.

S4



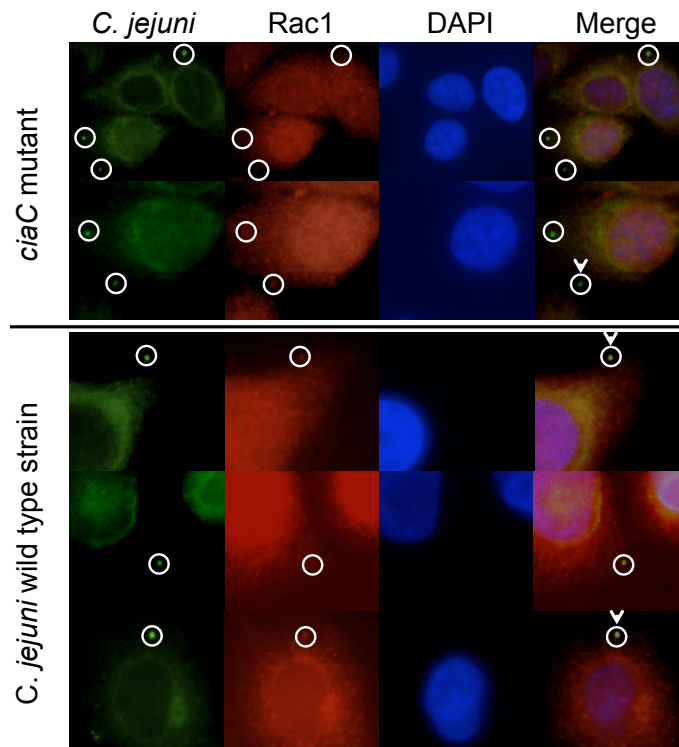
Supplemental Fig. S4. Treatment of INT 407 cells with vehicle has no effect on internalization of a *C. jejuni* wild-type strain. INT 407 cells were treated with the maximum volume of solvent used for delivery of inhibitors to host cells and inoculated with *C. jejuni* wild-type strain. Values represent the mean \pm standard deviation of internalized bacteria/well of a 24 well tissue culture plate. There was no statistical difference in *C. jejuni* binding to the INT 407 cells (not shown) (DMSO, $P = 0.85$, MeOH, $P = 0.55$) or internalization (DMSO, $P = 0.29$, MeOH, $P = 0.61$) observed for either vehicle.

S5



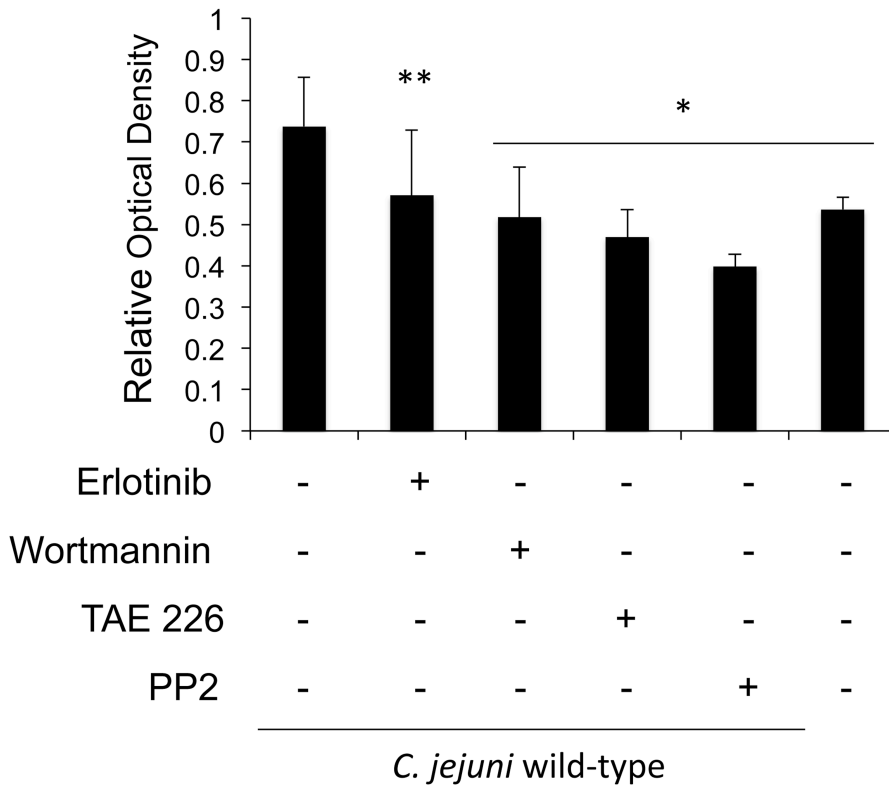
Supplemental Fig. S5. *C. jejuni* induces EGFR activation in a CadF FlpA dependent manner. INT 407 cells were infected with the *C. jejuni* wild-type strain and *C. jejuni cadF flpA* mutant. Panels: A) Proteins were immunoprecipitated from whole cell lysates with antibody reactive against total EGFR (α -EGFR MAb528). Blots were probed with an antibody that reacts against the active EGFR (pEGFR Tyr845 and Tyr1068) and an antibody that reacts against EGFR. B) Densitometric analysis of the level of EGFR activation of INT 407 cells inoculated with the wild-type isolate and *cadF flpA* mutant. The asterisks indicate a significance difference ($*P < 0.01$, $**P < 0.05$) in EGFR activation between cells inoculated with the wild-type isolate versus the *cadF flpA* mutant. The average background level in each lane was subtracted from the band of appropriate molecular weight and normalized to the cells only negative control. Values represent a fold change in activation over basal levels. Each condition was tested in triplicate on multiple days.

S6



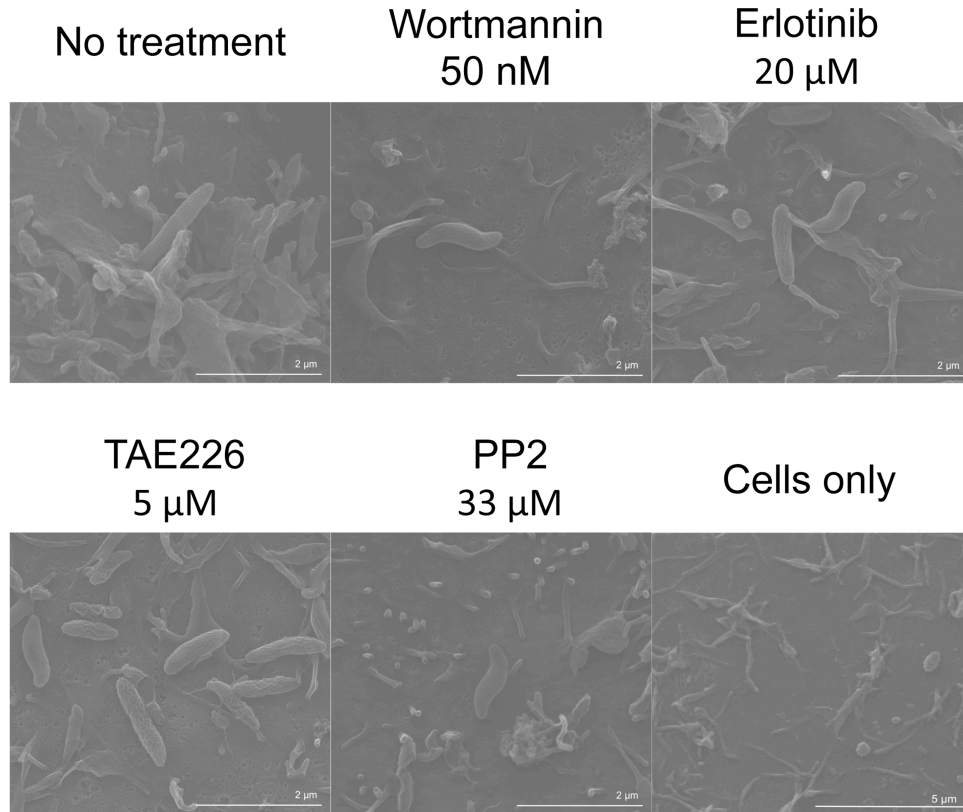
Supplemental Fig. S6. Additional evidence that Rac1 is recruited to sites of *C. jejuni* attachment. The localization of Rac1 in *C. jejuni*-infected cells was examined by immunofluorescence microscopy as outlined in “Experimental Procedures.” The cell-associated bacteria are indicated by the circles, whereas the *C. jejuni* adjacent to sites of accumulated Rac1 are indicated by the circles with the arrowhead. In contrast to the *C. jejuni* wild-type strain, fewer sites of Rac1 were observed in INT 407 cells inoculated with the *C. jejuni* *ciaC* mutant. The circles highlight the bound bacteria.

S7



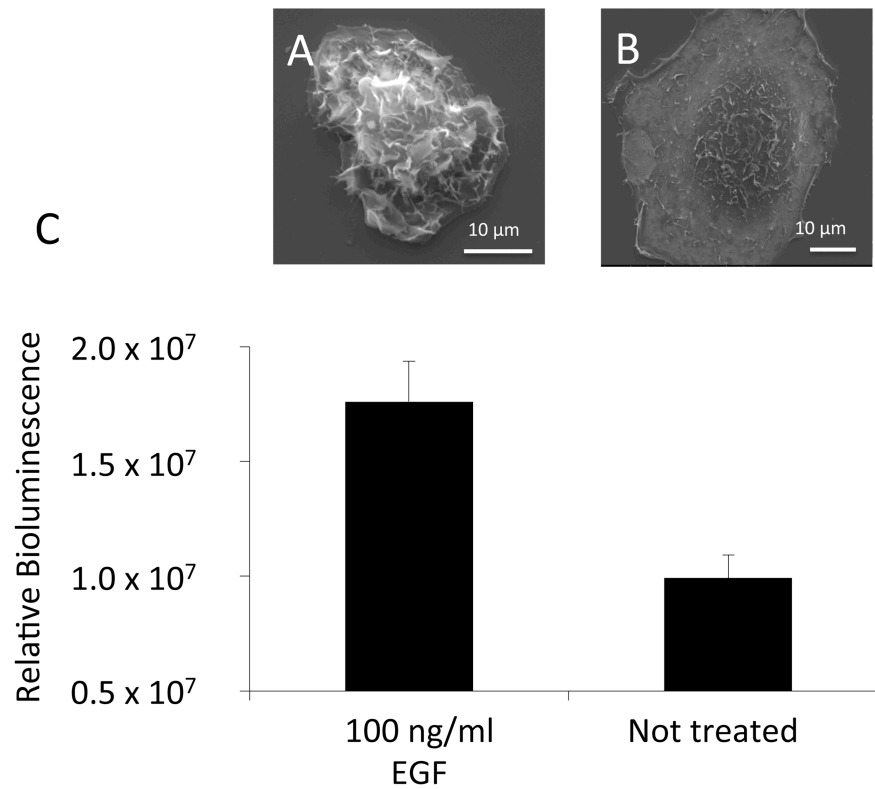
Supplemental Fig. S7. INT 407 cells inoculated with *C. jejuni* are deficient in Rac1 activation when pretreated with specific inhibitors of EGFR, FAK, PI3 kinase, or Src. Rac1 activation in cells inoculated with *C. jejuni* wild type strain following pretreatment with either 20 μ M erlotinib, 5 μ M TAE 226, 50 nM wortmannin, or 33 μ M PP2 for 30 minutes. Values represent at least 5 samples analyzed by GLISATM in duplicate. The asterisks indicate a significance difference ($*P < 0.01$, $**P < 0.05$) in Rac1 activation between untreated cells inoculated with the wild-type isolate versus each treatment group.

S8



Supplemental Fig. S8. INT 407 cells treated with inhibitors of EGFR, FAK, PI3 kinase or Src are deficient in membrane ruffling in response to *C. jejuni*. Scanning electron microscopy of INT 407 cells inoculated with *C. jejuni* wild type strain after pretreatment with the indicated inhibitors. Cell ruffling was enumerated and each drug treatment was found to significantly reduce ruffling when compared to the wild type strain ($P < 0.01$).

S9



Supplemental Fig. 9. INT 407 cells are responsive to the addition of EGF. Panels: A) Scanning electron microscopy (SEM) image of an INT 407 cell treated with 100 ng/ml of EGF for 2 minutes; B) SEM image of a non-treated INT 407 cell; C) Quantification of Rac1 activation by G-LISA™ in cells incubated for 2 minutes with 100 ng/ml of EGF versus untreated cells. The mean \pm standard deviation of total active Rac1 is indicated in Relative Bioluminescence.